

## Research Article

# Quantitative Proteomic Study of Human Lung Squamous Carcinoma and Normal Bronchial Epithelial Acquired by Laser Capture Microdissection

Xu Yan,<sup>1,2</sup> Cao Lan-Qin,<sup>3</sup> Jin Long-Yu,<sup>4</sup> Chen Zhu-Chu,<sup>1</sup> Zeng Gu-Qing,<sup>5</sup> Tang Can-E,<sup>1</sup> Li Guo-Qing,<sup>6</sup> Duan Chao-Jun,<sup>1</sup> Peng Fang,<sup>1</sup> Xiao Zhi-Qiang,<sup>1</sup> and Li Cui<sup>1</sup>

<sup>1</sup> Key Laboratory of Cancer Proteomics of Chinese Ministry of Health, Xiangya Hospital, Central South University, Changsha 410008, China

<sup>2</sup> Judicial Police General Hospital, Changsha 410004, China

<sup>3</sup> Department of Gynecology and Obstetrics, Xiangya Hospital, Central South University, Changsha 410008, China

<sup>4</sup> Department of Cardiothoracic Surgery, Third Xiangya Hospital, Central South University, Changsha 410013, China

<sup>5</sup> Department of General Introduction to Surgery, School of Medicine, University of South China, Hengyang 421001, China

<sup>6</sup> Department of Biology, School of Pharmacy and Life Science, University of South China, Hengyang 421001, China

Correspondence should be addressed to Li Cui, licuipwb@yahoo.com.cn

Received 8 June 2011; Revised 30 November 2011; Accepted 1 December 2011

Academic Editor: Kapil Mehta

Copyright © 2012 Xu Yan et al. This is an open access article distributed under the Creative Commons Attribution License, which permits unrestricted use, distribution, and reproduction in any medium, provided the original work is properly cited.

**Objective.** To investigate the differential protein profile of human lung squamous carcinoma (HLSC) and normal bronchial epithelium (NBE) and provide preliminary results for further study to explore the carcinogenic mechanism of HLSC. **Methods.** Laser capture microdissection (LCM) was used to purify the target cells from 10 pairs of HLSC tissues and their matched NHBE, respectively. A stable-isotope labeled strategy using iTRAQ, followed by 2D-LC/Q-STAR mass spectrometry, was performed to separate and identify the differential expression proteins. **Results.** A total of 96 differential expression proteins in the LCM-purified HLSC and NBE were identified. Compared with NBE, 49 proteins were upregulated and 47 proteins were downregulated in HLSC. Furthermore, the expression levels of the differential proteins including HSPB1, CKB, SCCA1, S100A8, as well as S100A9 were confirmed by western blot and tissue microarray and were consistent with the results of quantitative proteomics. **Conclusion.** The different expression proteins in HLSC will provide scientific foundation for further study to explore the carcinogenic mechanism of HLSC.

## 1. Introduction

Lung cancer ranks the first in the morbidity and mortality of human malignancies and keeps the leading position of all common malignant tumors worldwide. Histopathologically, lung cancers are classified into small cell lung cancer and nonsmall cell lung cancer. The latter is further classified into squamous cell carcinoma, adenocarcinoma, and large cell caicinoma, according to its morphologic patterns. Among which, squamous cell carcinoma is the most common, which accounts for 40%–70% [1]. Squamous cell carcinoma originates from the bronchial epithelial cell. Currently, the mechanism of the initiation, development, and dissemination of human lung squamous carcinomas (HLSCs) is still unclear.

Proteomics provides a new opportunity to reveal the carcinogenic mechanism of HLSC. The comparative proteomics compares the tumor and its origin tissue may reflect the carcinogenesis. However, the main obstacle for proteomics analysis is the heterogeneity of the soft tumor tissues. In order to improve the accuracy of the results, it is necessary to purify the target cells from the heterogeneous tissues. Laser capture microdissection (LCM) is one of the best technologies for cell purification [2–6]. The quantitative proteomics is one of the emerging fields for tumor proteomics study; isotope labeling relative and absolute quantification (iTRAQ) is a new technique in quantitative proteomics, which could be used to identify and quantify the protein expression levels and identify the small changes of protein expression in different tissues.

In this study, LCM was used to purify the target cells from HLSC tissues and matched NBE; iTRAQ followed by 2D-LC/Q-STAR mass spectrometry was performed to separate and identify the differential expression proteins in LCM-purified HLSC tissues and matched NHBE.

## 2. Materials and Methods

**2.1. Sample Collection, Laser Capture Microdissection, and Protein Extraction.** Twenty pairs of HSCL tissues and matched normal bronchial epithelium tissues from the LSCC patients undergoing curative surgery and receiving neither chemotherapy nor radiotherapy were obtained from Department of Cardiothoracic Surgery, The Second Xiangya Hospitals of Central South University, China. The patients signed an informed consent form for the study which was approved by the local ethical committee. Samples were diagnosed by histopathology. 10 pairs of the tissues were used for iTRAQ, and the other 10 pairs of the tissues for Western blotting, respectively. Tissues were frozen in  $-70^{\circ}\text{C}$ .

LCM was performed with a Leica AS LMD system to purify the interest cells from HSCL tissues and matched NBE tissues as previously described by us. Briefly, frozen sections (8 mm) from each HLSC and NBE tissues were prepared using a Leica CM 1900 cryostat (Leica) at  $-25^{\circ}\text{C}$ . The sections were placed on a membrane-coated glass slides (Leica), fixed in 75% alcohol for 30 s, and stained with 0.5% violet-free methyl green (Sigma). The stained sections were air-dried and then subjected to LCM.

The microdissected cells were dissolved in lysis buffer (7 M urea, 2 M thiourea, 65 mM DTT, 0.1 mM PMSF) at  $4^{\circ}\text{C}$  for 1 h and then centrifuged at 12 000 rpm for 30 min at  $4^{\circ}\text{C}$ . The supernatant was collected, and the protein concentration was determined by 2D Quantification kit (Amersham Biosciences). To diminish the effect of sample biological variation on the results of a proteomics analysis, equal amounts of proteins from the microdissected cells of 10 different individuals were pooled to generate one common sample iTRAQ labeling.

**2.2. Protein Digestion and Labeling with iTRAQ Reagents.** Trypsin digestion and iTRAQ labeling were performed according to the manufacturer's protocol (Applied Biosystems). Briefly, 100  $\mu\text{g}$  protein of each pooled sample was reduced and alkylated and then digested overnight at  $37^{\circ}\text{C}$  with trypsin (mass spectrometry grade; Promega) and labeled with iTRAQ reagents (Applied Biosystems) as follows: NBE, iTRAQ reagent 113; and HLSC, iTRAQ reagent 115. The labeled digests were then mixed and dried.

**2.3. Off-Line 2D LC-MS/MS.** The mixed peptides were fractionated by strong cation exchange (SCX) chromatography on a 20AD HPLC system (Shimadzu) using a polysulfoethyl column (2.1  $\times$  100 mm, 5  $\mu\text{m}$ , 300  $\text{\AA}$ ; The Nest Group Inc.) as previously described by us [7]. Briefly, the mixed peptides were desalted with Sep-Pak Cartridge (Waters), diluted with the loading buffer (10 mM  $\text{KH}_2\text{PO}_4$  in 25% ACN, pH 2.8), and loaded onto the column. Buffer A was identical in

composition to the loading buffer, and buffer B was same as buffer A except of containing 350 mM KCl. Separation was performed using a linear binary gradient of 0–80% buffer B in buffer A at a flow rate of 200  $\mu\text{l}/\text{min}$  for 60 min. The absorbance at 214 nm and 280 nm was monitored, and a total of 30 SCX fractions were collected along the gradient.

Each SCX fraction was dried down, dissolved in buffer C (5% ACN, 0.1% FA), and analyzed on Qstar XL (Applied Biosystems) as previously described by us [7]. Briefly, peptides were separated on a reverse-phase (RP) column (ZORBAX 300SB-C18 column, 5  $\mu\text{m}$ , 300  $\text{\AA}$ , 0.1  $\times$  15 mm; Micromass) using a 20AD HPLC system (Shimadzu). The HPLC gradient was 5–35% buffer D (95% ACN, 0.1% FA) in buffer C at a flow rate of 0.2  $\mu\text{l}/\text{min}$  for 65 min. Survey scans were acquired from 400 to 1800 with up to 4 precursors selected for MS/MS from  $m/z$  100–2000 using a dynamic exclusion of 30S. The iTRAQ-labeled peptides fragmented under CID conditions to give reporter ions at 113.1 and 1151 Th. The ratios of peak areas of the iTRAQ reporter ions reflect the relative abundances of the peptides and, consequently, the proteins in the samples. Larger, sequence-information-rich fragment ions were also produced under these MS/MS conditions and gave the identity of the protein from which the peptide originated.

**2.4. Data Analysis.** The ProteinPilot 3.0 software program (ABI, USA) was used to perform Protein identification and quantification analysis for the iTRAQ experiment. Identified proteins were grouped by the software to minimize redundancy; all peptides used for the calculation of protein ratios were unique to the given protein or proteins within the group. The protein confidence threshold cutoff for this study is ProtScore 1.3 (unused) with at least one peptide with 95% confidence. The relative protein abundances were analyzed by the signature ion ratio ( $m/z$ , 115/113): the ratio  $\geq 1.2$  and  $\leq 0.8$  as the differential expression proteins.

**2.5. Western Blotting.** Western blotting was performed in ten pairs of microdissected HLSC and NBE. Briefly, 30–50  $\mu\text{g}$  of purified protein was separated by 10% SDS-PAGE and transferred to PVDF membrane (Bio-Rad). The blots were incubated for 2 h at room temperature in TBST (20 mM Tris-Cl, 140 mM NaCl, pH 7.5, 0.05% Tween-20) containing 5% skim milk and then were incubated with monoclonal mouse anti-HSPB1 (dilution 1 : 1000, Abcam), monoclonal rabbit anti-CKB (dilution 1 : 200, Santa Cruze), polyclonal rabbit anti-human S100A8/A9, and polyclonal mouse anti-human SCCA1 (dilution 1 : 200, Santa Cruze) overnight at  $4^{\circ}\text{C}$ . After washing three times in TBST, membranes were incubated with a horse radish peroxidase conjugated secondary antibody (dilution 1 : 3,000, Amersham Biosciences) for 1 h at room temperature. The blots were developed using ECL detection reagent and quantitated by densitometry using ImageQuant image analysis system (Storm Optical Scanner). The  $\beta$ -actin was detected simultaneously as a loading control.

**2.6. Tissue Microarray and Immunohistochemistry.** The tissue microarray containing 30 lung squamous cell carcinoma,

TABLE 1: The clinicopathological parameters of the 100 tissue specimens.

Classification	Number
Gender	
Male	84
Female	16
Age	
≥55	68
<55	32
Histological type	
Squamous cell carcinoma	30
High differentiated	5
Moderately differentiated	14
Poorly differentiated	11
Adenocarcinoma	8
Large cell carcinoma	6
Small cell carcinoma	6
Lymph node metastasis	30
Positive	
Normal lung tissue	20

30 metastatic carcinoma, 20 normal lung tissues, and 20 other types of lung cancer (lung adenocarcinoma, large cell carcinoma, small cell carcinoma) was from AURAGENE. The detailed information of the tissues is provided in Table 1.

Serial sections (4  $\mu\text{m}$ ) were cut from the tissue microarray, deparaffinized, rehydrated, and treated with an antigen retrieval solution (10 mmol/L sodium citrate buffer, pH 6.0). Endogenous peroxidase was blocked using 3% hydrogen peroxide in methanol for 20 min. Nonspecific sites were blocked for 20 min using 1% normal serum in PBS. Sections were incubated for 2 h with a dilution of 1 : 200 polyclonal rabbit anti-human S100A8/A9 or SCCA1 and then were incubated with 1 : 1000 dilution of biotinylated secondary antibody followed by avidin-biotin peroxidase complex (DAKO) according to the manufacturer's instructions. Finally, tissue sections were incubated with 3', 3'-diaminobenzidine (Sigma) until a brown color developed and counterstained with Harris' modified hematoxylin. In negative controls, primary antibodies were omitted.

**2.7. Evaluation of Staining.** Immunostaining was blindly evaluated by two observers in an effort to provide a consensus on staining patterns. Each case was rated according to a score that added a scale of intensity of staining to the area of staining. At least 10 high-power fields were chosen randomly, and >1000 cells were counted for each section. The positive intensity of staining was graded on the following scale: 0, no staining; 1+, pale yellow stained; 2+, tan-yellow stained; and 3+, brown stained. The negative intensity of staining was evaluated as follows: 0, <5% of tissue stained negative; 1+, 5%–25% of tissue stained negative; 2+, between 25% and 50% stained negative; 3+, 50%–75% stained negative; and 4+, >75% stained negative. The minimum score when

summed (positive stained + negative stained) was therefore 2 and the maximum, 7. A combined staining score (positive stained + negative stained) of <2 was considered to be negative staining (–); a score between 2 and 3 was considered to be weak staining (+); between 3 and 6 was considered to be moderate staining (++); and between 6 and 7 was considered to be strong staining (+++).

**2.8. Statistical Analysis.** One-way analysis of variance (ANOVA) and LSD analysis (SPSS 12.0) were used in this study. All statistical tests were two-sided. Differences were considered statistically significant for  $P$  values < 0.05.

### 3. Results

**3.1. Identification of Differentially Expressed Proteins in HLSC and NBE Using iTRAQ Labeling and 2D LC-MS/MS.** A total of 96 differentially expressed proteins were identified by iTRAQ labeling and 2D LC-MS/MS, among which 49 up-regulated and 47 downregulated proteins in HLSC (Table 2). MS/MS spectrum used for the identification and quantitation of CKB is shown in Figure 1.

Biological functions and subcellular location of the identified 96 proteins were searched in EMBL-EBI and EXPASY database. The most common differential expression proteins were located in the cytoplasm, followed by nuclear proteins, secreted proteins, and mitochondrial proteins. The locations of the proteins were concomitant with their functions, which were structural proteins, metabolic enzymes, signal transduction proteins, cell adhesion, and proliferation-related proteins (Figure 2).

**3.2. Validation of Differentially Expressed Proteins Identified by Proteomics.** Five proteins (HSPB1, S100A8/A9, CKB, and SCCA1) identified by MS analysis were chosen for verification. Western blotting was performed to detect the expression levels of the four proteins in 10 cases of LCM-purified NBE and HLSC. As shown in Figure 3, HSPB1 and S100A8/A9 were upregulated, whereas CKB and SCCA1 were downregulated in the HLSC versus NBE ( $P < 0.05$ ), which is consistent with the findings in MS analysis.

**3.3. Detection of the Expression of the Differential Proteins by TMA and Immunohistochemistry.** The expressions of SCCA1, S100A8/A9 in 30 squamous cell carcinoma, 30 metastatic carcinoma, and 20 nonsquamous cell carcinoma (8 adenocarcinoma, 6 large cell carcinoma, 6 small cell carcinoma) were detected by TMA and immunohistochemistry. As shown in Figure 4 and Table 3, the expressions of SCCA1 in lung squamous cell carcinoma, other types of lung carcinoma, and metastatic carcinoma were lower than those in normal lung tissue ( $P < 0.05$ ). As shown in Figure 5 and Table 4, S100A8/A9 was expressed in all types of lung cancer and normal tissues. Yet, the expression of S100A8 in lung squamous cell carcinoma was stronger than that in normal tissues and other types of lung cancer tissues ( $P < 0.05$ ). As shown in Figure 6 and Table 5, the expression of S100A9 in cancer tissues including lung squamous cell carcinoma,

TABLE 2: Differential expressed proteins in LCM-purified HLSC and NHBE identified by mass spectrometry.

No. of proteins	Coverage (%)	UniprotKB	AC	Name	Peptides	115 : 113
1	62.34	IPI00554648.3	P05787	KRT8	60	0.4098
2	60.05	IPI00479145.2	P08727	KRT19	51	0.6193
3	56.53	IPI00745872.2	P02768	ALB	40	0.5735
4	59.8	IPI00009867.3	P13647	KRT5	68	0.7839
5	54.17	IPI00019502.3	P35579	MYH9	32	1.6587
6	39.41	IPI00007752.1	P68371	TUBB2C	37	0.1989
7	35.87	IPI00784154.1	P10809	HSPD1	30	1.5497
8	34.28	IPI00479186.5	P14618	PKM2	21	1.5827
9	34.2	IPI00844215.1	Q13813	SPTAN1	17	0.5947
10	42.7	IPI00450768.7	Q04695	KRT17	25	0.7824
11	30.05	IPI00219018.7	P04406	GAPDH	22	1.5761
12	28.96	IPI00845339.1	P08107	HSPA1A/1B	15	0.5216
13	27.82	IPI00022204.2	P29508	SERPINB3	16	0.3215
14	31.05	IPI00554788.5	P05783	KRT18	32	0.5866
15	50.34	IPI00300725.7	P02538	KRT6A	59	1.6359
16	24.25	IPI00553177.1	P01009	SERPINA1	13	0.651
17	23.08	IPI00654755.3	P68871	HBB	19	1.4246
18	22.65	IPI00455383.4	Q00610	CLTC	12	0.6788
19	23.9	IPI00003362.2	P11021	HSPA5	13	1.9385
20	20.99	IPI00025252.1	P30101	PDIA3	14	1.477
21	19.32	IPI00218914.5	P00352	ALDH1A1	11	0.3403
22	35.01	IPI00217963.3	P08779	KRT16	19	1.7771
23	18.49	IPI00872684.1	P15311	EZR	9	0.3327
24	16.7	IPI00013808.1	O43707	4ACTN4	14	0.4979
25	33.95	IPI00290077.1	P19012	KRT15	20	0.6399
26	16	IPI00219757.13	P09211	GSTP1	13	0.5584
27	15.06	IPI00000105.4	Q14764	MVP	7	0.516
28	14.96	IPI00645078.1	P22314	UBA1	8	1.345
29	14.66	IPI00788802.1	P29401	TKT	8	1.4856
30	13.96	IPI00020599.1	P27797	CALR	7	2.1548
31	13.57	IPI00169383.3	P00558	PGK1	8	0.6459
32	13.23	IPI00887678.1		LOC654188	8	2.2579
33	12.44	IPI00640741.1	Q06830	PRDX1	6	6.5599
34	12.12	IPI00604620.3	P19338	NCL	7	1.5576
35	12.1	IPI00893881.1	Q53G64	AGR2	14	0.4388
36	11.27	IPI00853068.1	Q86YQ1	HBA	11	1.372
37	11.23	IPI00816252.1		H2BFS	18	1.4498
38	11.14	IPI00657682.2	P08263	GSTA1	6	0.2536
39	11.01	IPI00643384.2	A6NLG9	BGN	5	0.2803
40	23.25	IPI00550661.2	P13646	KRT13	20	2.3013
41	38.63	IPI00384444.5	P02533	KRT14	19	1.448
42	10.4	IPI00027497.5	P06744	GPI	4	2.4216
43	9.95	IPI00027462.1	P06702	S100A9	7	3.1824
44	9.85	IPI00215948.4	P35221	CTNNA1	5	0.6596
45	9.76	IPI00453473.6	P62805	HIST1H4I	5	15.7322
46	9.42	IPI00794543.1	A8K1M2-cDNA	FLJ75174	4	0.3772
47	9.08	IPI00549248.4	P06748	NPM1	9	2.033
48	8.97	IPI00221226.7	P08133	ANXA6	4	0.6198
49	8.63	IPI00032140.4	P50454	SERPINH1	4	2.9965

TABLE 2: Continued.

No. of proteins	Coverage (%)	UniprotKB	AC	Name	Peptides	115 : 113
50	8.55	IPI00025512.2	P04792	HSPB1	20	3.9981
51	8.14	IPI00798430.1	Q53H26	TF	4	0.6764
52	35.45	IPI00011654.2	P07437	TUBB	28	1.5243
53	8	IPI00022977.1	P12277	CKB	4	0.41
54	7.84	IPI00307162.2	P18206	VCL	5	2.4223
55	7.22	IPI00295400.1	P23381	WARS	3	1.4314
56	6.92	IPI00792011.1	Q8NF12	CAPS	5	0.3241
57	6.36	IPI00013415.1	P62081	RPS7	3	3.2407
58	6.27	IPI00025465.1	P20774	OGN	4	0.1986
59	6.24	IPI00853455.1	C9JIH9	CTSD	4	0.639
60	6.19	IPI00152295.1	Q8TC71	SPATA18	3	0.4421
61	9.34	IPI00829767.1	P01859	IGHG2	4	0.6251
62	6	IPI00789551.1	A8MXP9	MATR3	5	2.0326
63	6	IPI00871851.1	Q15019	SEPT2	4	1.3502
64	6	IPI00291006.1	P40926	MDH2	3	1.924
65	6	IPI00795633.1	Q8IWL5	CLU	3	0.3392
66	5.95	IPI00423462.5	Q6N092	IGHA1	3	0.7002
67	8.33	IPI00007047.1	P05109	S100A8	5	2.1281
68	5.73	IPI00654709.1	Q6PKA6	ALDH3A1	3	0.431
69	4.72	IPI00294834.6	Q12797	ASPH	2	2.3432
70	6.6	IPI00027350.3	P32119	PRDX2	3	1.7333
71	4.45	IPI00025086.3	P20674	COX5A	2	1.4661
72	4.4	IPI00009032.1	P05455	SSB	2	0.6693
73	4.4	IPI00060715.1	Q96CX2	KCTD12	2	0.7126
74	4.31	IPI00646059.1	Q5VXV2	SET	2	2.3791
75	4.13	IPI00216308.5	P21796	VDAC1	2	0.4488
76	4.08	IPI00032179.2	P01008	SERPINC1	2	0.6734
77	4.01	IPI00025796.3	O75489	NDUFS3	2	0.6022
78	4	IPI00020042.2	P43686	PSMC4	2	0.603
79	4	IPI00011126.6	P62191	PSMC1	2	0.6418
80	3.71	IPI00883950.1	Q8TB01	CKAP4	2	2.3486
81	2.95	IPI00420014.2	O75643	ASCC3L1	1	1.6656
82	2.73	IPI00003944.1	P11182	DBT	1	0.5156
83	2.58	IPI00479786.4	Q92945	KHSRP	1	1.9958
84	2.38	IPI00419237.3	P28838	LAP3	1	1.7329
85	2.34	IPI00024933.3	P30050	RPL12	1	1.7853
86	2.19	IPI00219221.3	P47929	LGALS7	1	0.7374
87	2.02	IPI00444204.1	Q6ZS74	ALB	1	2.0254
88	2.02	IPI00847322.1	Q4ZJ11	SOD2	1	0.6501
89	2.01	IPI00745729.2	A6PVW9	SELENBP1	1	0.5016
90	2.01	IPI00375746.4	Q6ZN66	GBP6	1	4.68
91	2	IPI00413654.3	Q13243	SFRS5	1	4.0553
92	2	IPI00010133.3	P31146	CORO1A	1	1.5283
93	2	IPI00221222.7	P53999	SUB1	1	7.5809
94	2	IPI00024976.5	Q9NS69	TOMM22	1	2.5511
95	2	IPI00888660.1		SDHA	1	2.0706
96	2	IPI00013895.1	P31949	S100A11	2	0.6028

Differentially labeled proteins are identified by QSTAR. The % coverage of analyzed peptides and Swiss-Prot accession number were shown for each protein. Proteins displaying an average fold-difference of  $\geq 1.2$ -fold up- (+) or  $\leq 0.8$ -fold down- (-) regulation between pairs of conditions where  $P < 0.05$  are shown (115: the group of HLSC; 113: the group of NHBE).

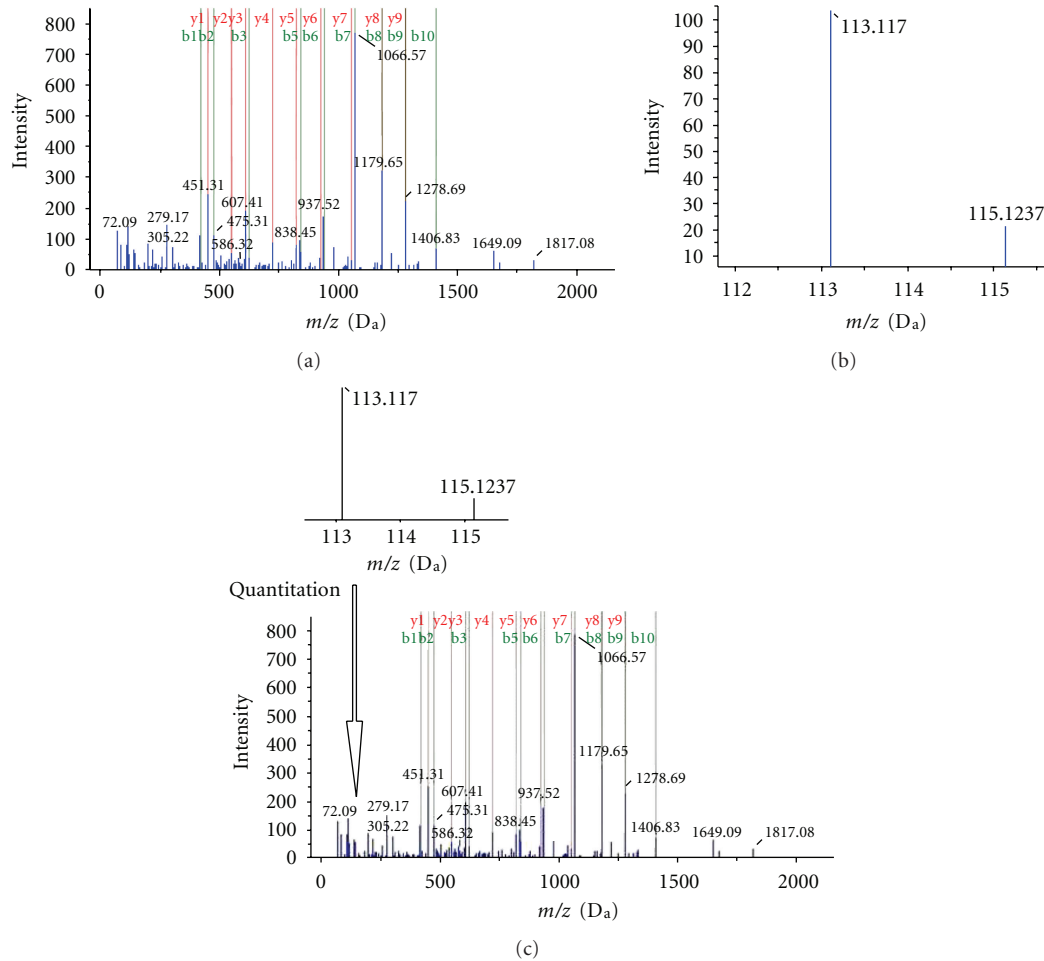


FIGURE 1: The fragment ion spectra of peptide sequence tag (PST) from CKB protein, highlighting the relative abundances of overexpression in NHBE. The ion assignments are as follows: 113: NHBE; and 115: HLSC.

metastatic carcinoma, and other types of lung cancer was stronger than in normal tissues ( $P < 0.05$ ).

#### 4. Discussion

Recently, numerous successful explorations about carcinogenic molecular mechanisms of HLSC on gene and transcription were reported. Compared with genome and transcriptome, which is relatively static and will be transcribed into a variety of functionally distinct proteins, proteome may provide a more realistic picture of function aberrations in cancer cells. Proteomics has become the frontier era of the postgenomic; the new methods and achievements are emerging in large number. Traditional 2-DE technique has been used widely for comparative proteomics with a significant achievement, but also there is disadvantagedness. iTRAQ quantitative proteomics can overcome that deficiencies (such as identified membrane proteins) and increase the number and types of differential expression proteins. In contrast to 2-DE, iTRAQ technology has a better repeatability and quantification.

In the study, LCM was used to purify the target cells from HLSC tissues and matched NHBE, respectively. A stable

isotope-labeled strategy using iTRAQ, followed by 2D-LC/Q-STAR mass spectrometry, was performed to separate and identify the differential expression proteins. A total of 96 differential expression proteins in the LCM-purified HLSC and NHBE were identified.

Among the differential expression proteins, HSPB1 (HSP27) is heat shock protein family member, which has important biological functions, a chaperone protein involved in regulation of cell proliferation, differentiation, apoptosis and signal transduction, and so forth. Induced epithelial-mesenchymal transition (EMT) in human lung cancer cells (adenocarcinoma cells), HSPB1, was high-regulated and involved in the regulation of cell migration, adhesion and invasion [8]. In the colon, prostate, and breast cancer, HSPB1 expression was associated with tumor occurrence and metastasis. HSPB1 was high-regulated, suggesting the poor prognosis and resistance to drugs [9–12]. Guo et al. found that the functional HSPB1 promoter  $-1271G > C$  variant may affect lung cancer susceptibility and survival by modulating endogenous HSPB1 synthesis levels [13]. The research showed HSPB1 protein and its phosphorylation increased in parallel with enhanced metastatic potentials of hepatocellular carcinoma (HCC) cells; HSPB1 knockdown significantly

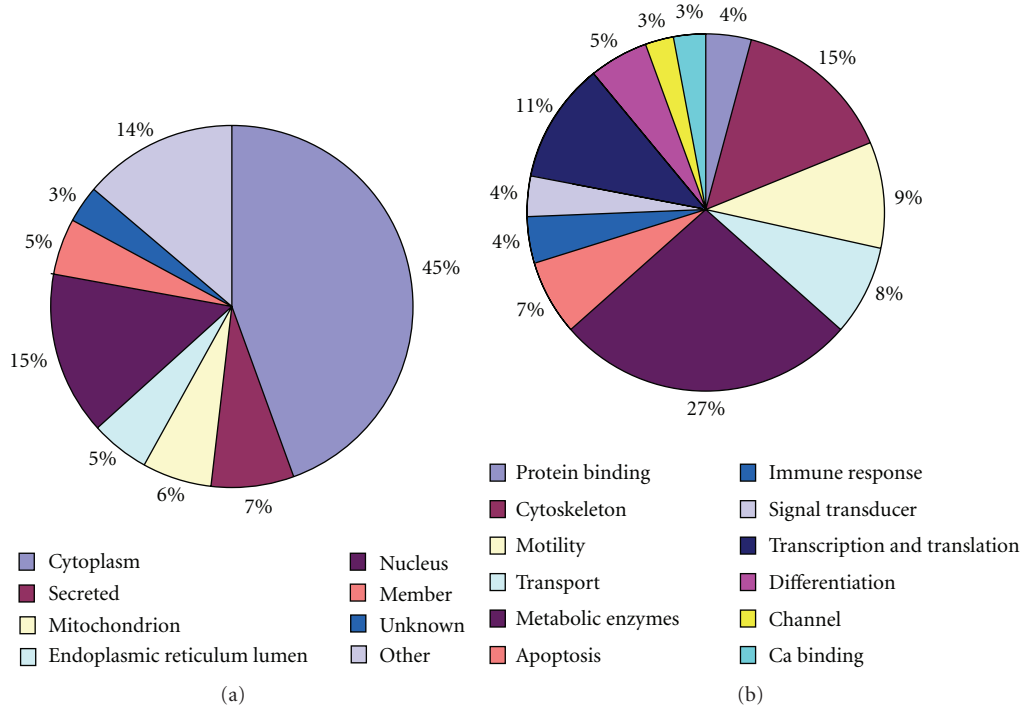


FIGURE 2: Biological functions and subcellular location of the identified 96 proteins. (a) A pie chart representing the distribution of the identified 96 proteins according to their cellular locations; (b) A pie chart representing the distribution of the identified 96 proteins according to their biological function.

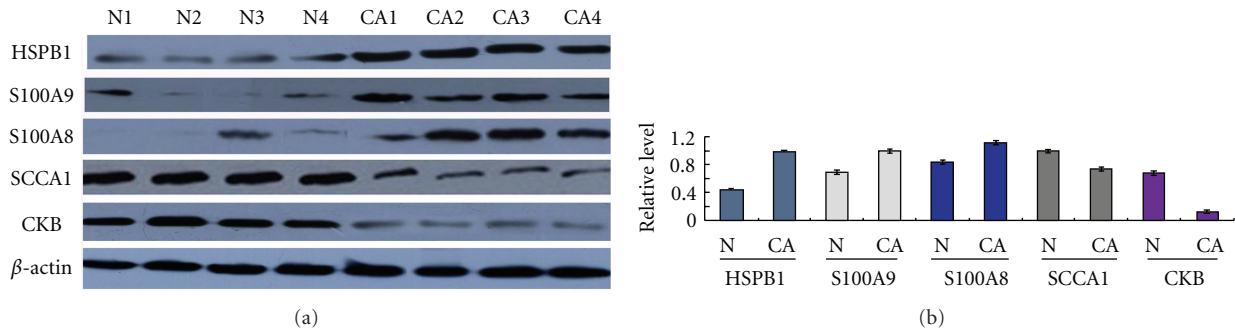


FIGURE 3: Representative results of Western blotting analysis of HSPB1, CKB, S100A8/A9, and SCCA1 in HLSC (CA) and NHBE (N).  $\beta$ -actin was used as a loading control.

TABLE 3: SCCA1 expression in various tissues by IHC.

Classification	Number	—	+	++-+++	P value
Squamous cell carcinomas	30	21	5	4	0.038 <sup>a</sup>
High differentiated	3	3	0	0	0.406 <sup>b</sup>
Moderately differentiated	11	9	2	0	
Poorly differentiated	10	6	2	2	
Normal lung tissue	20	9	10	1	
Metastatic carcinoma	29	16	5	8	0.029 <sup>c</sup>
Other types	20	12	6	2	0.001 <sup>d</sup>

<sup>a</sup> $P < 0.05$  by LSD, squamous cell carcinomas versus normal lung tissue. <sup>b</sup> $P > 0.05$  by ANOVA, high differentiated versus moderately versus poorly. <sup>c</sup> $P < 0.05$  by LSD, metastatic carcinoma versus normal lung tissue. <sup>d</sup> $P < 0.05$  by LSD, other types versus normal lung tissue.

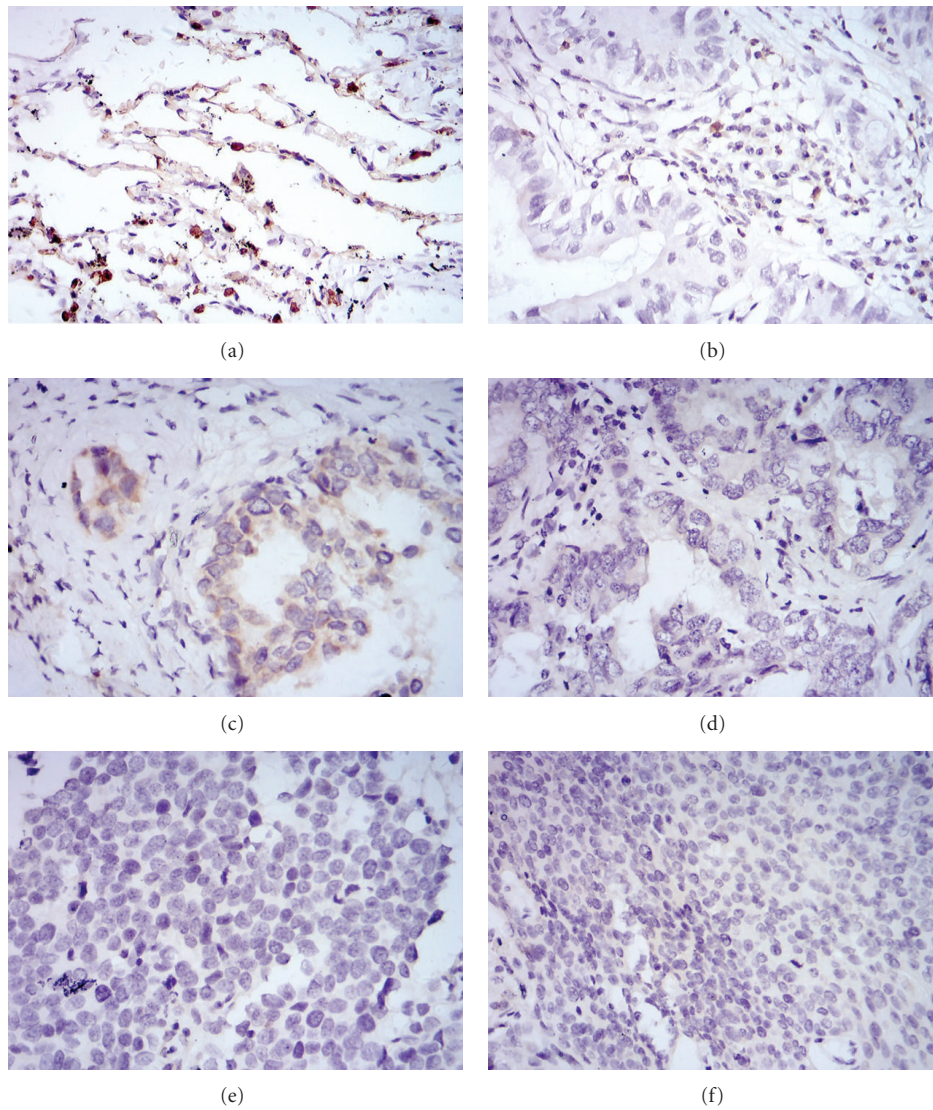


FIGURE 4: Immunohistochemistry staining in tissue chip of SCCA1 protein expression in lung cancer tissue and normal tissues ((a) normal lung tissue, (b) lung squamous cell carcinomas, (c) metastatic carcinoma, (d) adenocarcinoma, (e) small cell carcinoma, (f) large cell carcinoma tissues).

TABLE 4: S100A8 expression in various tissues by IHC.

Classification	Number	—	+	++-+++	<i>P</i> value
Squamous cell carcinomas	30	1	5	24	0.000 <sup>a</sup>
High differentiated	3	0	0	3	0.705 <sup>b</sup>
Moderately differentiated	11	2	7	2	
Poorly differentiated	10	6	2	2	
Normal lung tissue	20	1	11	8	
Metastatic carcinoma	29	0	11	18	0.007 <sup>c</sup>
Other types	20	3	12	5	0.000 <sup>d</sup>

<sup>a</sup>*P* < 0.05 by LSD, squamous cell carcinomas versus normal lung tissue. <sup>b</sup>*P* > 0.05 by ANOVA, high differentiated versus moderately versus poorly. <sup>c</sup>*P* < 0.05 by LSD, metastatic carcinoma versus normal lung tissue. <sup>d</sup>*P* < 0.05 by LSD, other types versus normal lung tissue.



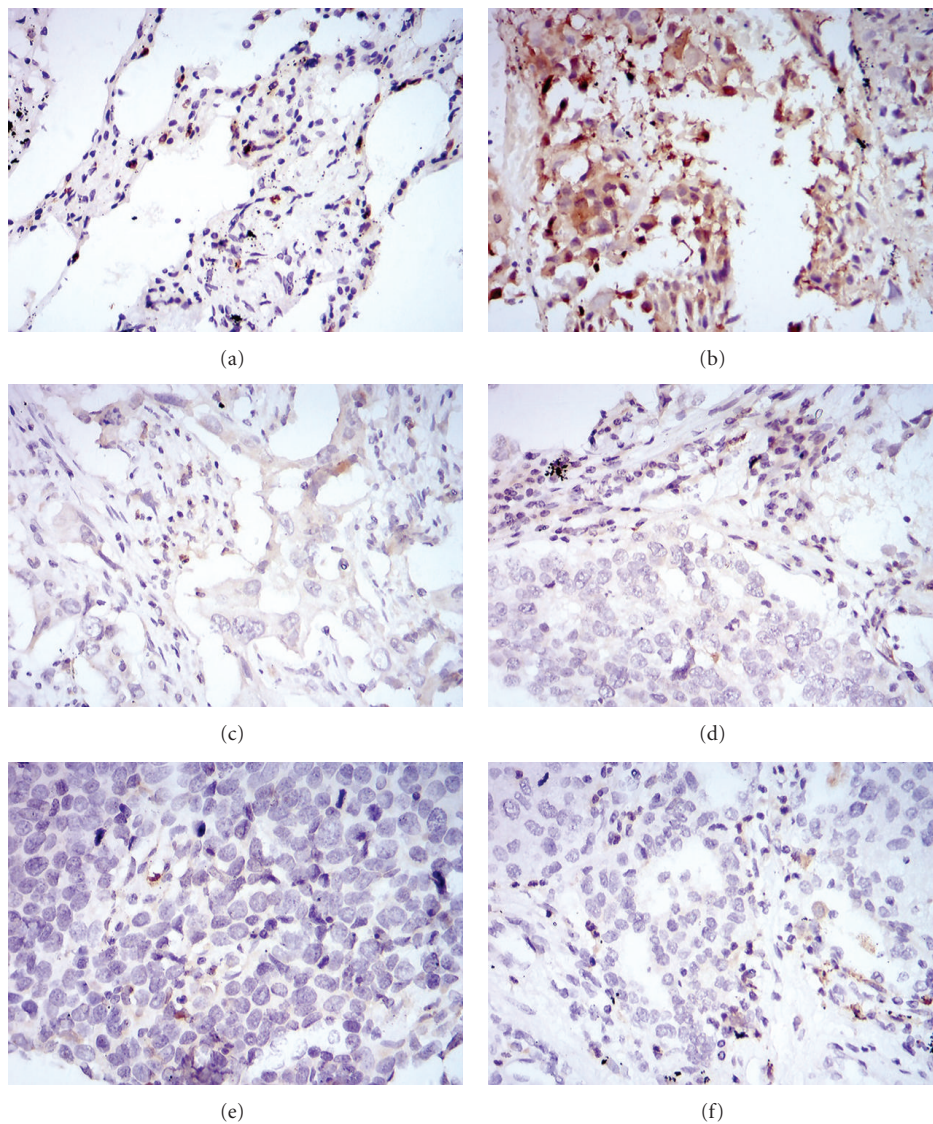


FIGURE 5: Immunohistochemistry staining in tissue chip of S100A8 protein expression in lung cancer tissue and normal tissues ((a) normal lung tissue, (b) lung squamous cell carcinomas, (c) metastatic carcinoma, (d) adenocarcinoma, (e) small cell carcinoma, (f) large cell carcinoma tissues).

TABLE 5: S100A9 expression in various tissues by IHC.

Classification	Number	—	+	++-+++	Pvalue
Squamous cell carcinomas	30	0	2	28	0.01 <sup>a</sup>
High differentiated	3	0	3	0	0.705 <sup>b</sup>
Moderately differentiated	11	9	2	0	
Poorly differentiated	10	8	2	0	
Normal lung tissue	20	0	10	10	
Metastatic carcinoma	29	0	4	25	0.000 <sup>c</sup>
Other types	20	0	2	18	0.000 <sup>d</sup>

<sup>a</sup> $P < 0.05$  by LSD, squamous cell carcinomas versus normal lung tissue. <sup>b</sup> $P > 0.05$  by ANOVA, high differentiated versus moderately versus poorly. <sup>c</sup> $P < 0.05$  by LSD, metastatic carcinoma versus normal lung tissue. <sup>d</sup> $P < 0.05$  by LSD, other types versus normal lung tissue.

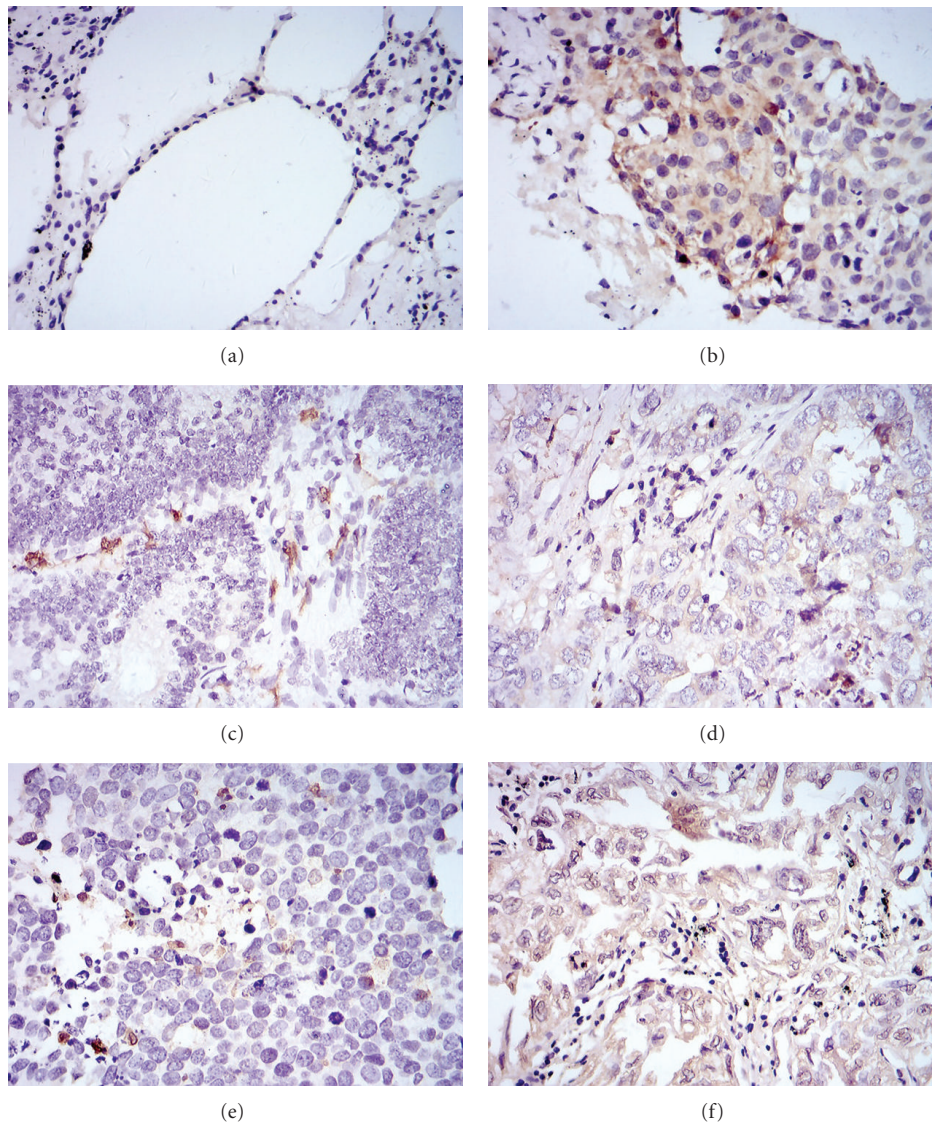


FIGURE 6: Immunohistochemistry staining in tissue chip of S100A9 protein expression in lung cancer tissue and normal tissues ((a) normal lung tissue, (b) lung squamous cell carcinomas, (c) metastatic carcinoma, (d) adenocarcinoma, (e) small cell carcinoma, (f) large cell carcinoma tissues).

suppressed cells migration and invasion and induced cell apoptosis [14]. Ye et al. showed that upregulated HSPB1 expression was potentially involved in human oral squamous cell carcinoma growth and metastasis [15]. In our study, HSPB1 was upregulated in HLSC compared with NHBE, confirmed by Western blot analysis. It was suggested that HSPB1 might play a certain role in carcinogenic of HLSC.

CKB (creatinekinase B) is a member of the creatine kinase family, that exists widely in skeletal muscle, myocardial, nerve tissue, and mitochondria. CKB participated in energy signaling pathways and catalyzed phosphate group reversibly from creatine phosphate to ADP to generate ATP and creatine. CKB expressed in the organization demanded high energy, as a nuclear “energy supplier”. CKB was downregulated protein in human prostate cancer cells associated with progression [16]. Reduced expression has been reported in colon, and renal cancer compared with matched adjacent

normal tissues [17, 18]. Our finding of reduced levels of CKB in human lung squamous carcinoma suggests a novel association for CKB with HLSC which needs to be investigated further.

SCCA1 (Squamous cell carcinoma antigen 1) also named SERPINB3 (serine protease inhibitor3) belonged to serine protease inhibitor family, that was physiologically found in normal squamous epithelium but overexpressed in squamous cell carcinoma (lung, cervical, esophagus, etc.). The biological role of this serpin in carcinogenesis has not been defined. On the one hand, SCCA1 can decrease NK tumour invasion [19] and inhibit apoptosis by inhibiting P38 phosphorylation and release of C cytochromes [20, 21]. Elevated levels of SCCA1 have been reported in liver, esophagus, mammary carcinoma, and so forth, associated with malignant cancer, prognosis, and recurrence [22]. In a previous study, it was reported that SCCA1 expression levels

were associated with tumor progression. Increasing number of reports suggests that SCCA has been implicated as a tumor marker for squamous [23]. Interestingly, our finding is that SCCA1 levels were downregulated in human lung squamous carcinoma compared with corresponding normal tissue. Our laboratory reported that SCCA1 levels were downregulated in nasopharyngeal carcinoma by promoter methylation [24]. Whether lung squamous carcinoma exists in promoter methylation, further analysis of the expression of SCCA1 in preneoplastic lesions for squamous cell carcinoma of the lung is needed.

Heterodimer S100A8/A9 is the member of calcium-binding protein S100 protein family, the inflammation factor, and inhibition of casein kinase I, II activity. Physically, S100A8/A9 is expressed as the early stages of cell differentiation in bone marrow and granulocytes and monocytes in circulation. Some inflammatory diseases, such as rheumatoid arthritis, inflammatory bowel disease, chronic pneumonia, their epithelial cells, and the cells of inflammatory exudate in early stage of inflammatory diseases express S100A8/A9. Elevated levels of S100A8/A9 have been reported in lung, stomach, breast, pancreatic, prostate cancer, and so forth. In addition, S100A9 has correlation with the poor differentiation of breast, lung, and thyroid cancer [7, 25–27]. Iikawa reveals a novel role for myeloid-derived S100A8/A9 in activating MAPK and NF- $\kappa$ B signaling pathways associated with colon tumorigenesis and in promoting tumor growth and metastasis [28]. Our findings are consistent with the reported that S100A8/A9 is upregulated in human lung squamous carcinoma compared with corresponding normal tissue. Although many possible functions have been proposed for S100A8/A9, its biological role still remains to be defined.

## 5. Conclusions

In conclusion, our data suggest that the several differential expression proteins may play a key role in human lung squamous carcinoma. Known to that during the development of human lung squamous cell carcinoma, bronchial epithelial cells exhibit a progressive series of morphologically distinct changes: hyperplasia, squamous metaplasia, dysplasia, carcinoma in situ, and finally invasive squamous cell carcinoma. We seek to identify differential expression proteins that can be used to monitor these premalignant changes under the assumption that these morphologic changes are accompanied by abnormal expression proteins. Thus, additional research using a larger number of tumor specimens is needed to confirm our findings more assuredly and we will make greater efforts to elucidate the precise molecular mechanisms of how the protein acts on the carcinogenesis in future works.

## Author's Contribution

X. Yan, C. Lan-Qin, and J. Long-Yu contributed equally to this work.

## Acknowledgments

This work is supported by the National Natural Science Foundation of China (no. 30972970), Program for New Century Excellent Talents in University (2007-0861), Nature Scientific Foundation of Hunan Province (08JJ6010), and Scientific Research Foundation of Department of Public Health of Hunan Province (B2007-068; B2010-037); Scientific Research Fund of Department of Education of Hunan Province (09C837), China.

## References

- [1] A. D. Lopez, "Counting the dead in China measuring tobacco impact in the developing world," *BMJ*, vol. 317, no. 170, pp. 1399–1400, 1998.
- [2] R. F. Bonner, M. Emmert-Buck, K. Cole et al., "Laser capture microdissection: molecular analysis of tissue," *Science*, vol. 278, no. 5342, pp. 1481–1491, 1997.
- [3] A. R. Shekhouh, C. C. Thompson, W. Prime et al., "Application of laser capture microdissection combined with two-dimensional electrophoresis for the discovery of differentially regulated proteins in pancreatic ductal adenocarcinoma," *Proteomics*, vol. 3, no. 10, pp. 1988–2001, 2003.
- [4] C. Li, Y. Hong, Y. X. Tan et al., "Accurate qualitative and quantitative proteomic analysis of clinical hepatocellular carcinoma using laser capture microdissection coupled with isotope-coded affinity tag and two-dimensional liquid chromatography mass spectrometry," *Molecular and Cellular Proteomics*, vol. 3, no. 4, pp. 399–409, 2004.
- [5] H. Neubauer, S. E. Clare, R. Kurek et al., "Breast cancer proteomics by laser capture microdissection, sample pooling, 54-cm IPG IEF, and differential iodine radioisotope detection," *Electrophoresis*, vol. 27, no. 9, pp. 1840–1852, 2006.
- [6] V. Patel, B. L. Hood, A. A. Molinolo et al., "Proteomic analysis of laser-captured paraffin-embedded tissues: a molecular portrait of head and neck cancer progression," *Clinical Cancer Research*, vol. 14, no. 4, pp. 1002–1014, 2008.
- [7] K. Arai, T. Teratani, R. Kuruto-Niwa, T. Yamada, and R. Nozawa, "S100A9 expression in invasive ductal carcinoma of the breast: S100A9 expression in adenocarcinoma is closely associated with poor tumour differentiation," *European Journal of Cancer*, vol. 40, no. 8, pp. 1179–1187, 2004.
- [8] V. G. Keshamouni, G. Michailidis, C. S. Grasso et al., "Differential protein expression profiling by iTRAQ-2DLC-MS/MS of lung cancer cells undergoing epithelial-mesenchymal transition reveals a migratory/invasive phenotype," *Journal of Proteome Research*, vol. 5, no. 5, pp. 1143–1154, 2006.
- [9] C. Garrido, A. Fromentin, B. Bonnotte et al., "Heat shock protein 27 enhances the tumorigenicity of immunogenic rat colon carcinoma cell clones," *Cancer Research*, vol. 58, no. 23, pp. 5495–5499, 1998.
- [10] C. Garrido, P. Mehlen, A. Fromentin et al., "Inconstant association between 27-kDa heat-shock protein (Hsp27) content and doxorubicin resistance in human colon cancer cells: the doxorubicin-protecting effect of Hsp27," *European Journal of Biochemistry*, vol. 237, no. 3, pp. 653–659, 1996.
- [11] D. R. Ciocca and L. M. Vargas-Roig, "Hsp27 as a prognostic and predictive factor in cancer," *Progress in Molecular and Subcellular Biology*, vol. 28, pp. 205–218, 2002.
- [12] P. Rocchi, A. So, S. Kojima et al., "Heat shock protein 27 increases after androgen ablation and plays a cytoprotective

- role in hormone-refractory prostate cancer,” *Cancer Research*, vol. 64, no. 18, pp. 6595–6602, 2004.
- [13] H. Guo, Y. Bai, P. Xu et al., “Functional promoter -1271G>C variant of HSPB1 predicts lung cancer risk and survival,” *Journal of Clinical Oncology*, vol. 28, no. 11, pp. 1928–1935, 2010.
- [14] K. Guo, N. X. Kang, Y. Li et al., “Regulation of HSP27 on NF- $\kappa$ B pathway activation may be involved in metastatic hepatocellular carcinoma cells apoptosis,” *BMC Cancer*, vol. 9, article 100, 2009.
- [15] H. Ye, A. Wang, B.-S. Lee et al., “Proteomic based identification of manganese superoxide dismutase 2 (SOD2) as a metastasis marker for oral squamous cell carcinoma,” *Cancer Genomics and Proteomics*, vol. 5, no. 2, pp. 85–93, 2008.
- [16] A. Glen, C. S. Gan, F. C. Hamdy et al., “ITRAQ-facilitated proteomic analysis of human prostate cancer cells identifies proteins associated with progression,” *Journal of Proteome Research*, vol. 7, no. 3, pp. 897–907, 2008.
- [17] R. Tom, T. Lauren, M. Damien, B. S. Lee, and R. V. Benya, “Consequence of gastrin-releasing peptide receptor activation in a human colon cancer cell line: a proteomic approach,” *Journal of Proteome Research*, vol. 5, no. 6, pp. 1460–1468, 2006.
- [18] K. W. Michael, V. D. Leroi, S. Andreas et al., “Differential protein expressions in renal cell carcinoma: new biomarker discovery by mass spectrometry,” *Journal of Proteome Research*, vol. 8, no. 8, pp. 3797–3807, 2009.
- [19] Y. Suminami, S. Nagashima, A. Murakami et al., “Suppression of a squamous cell carcinoma (SCC)-related serpin, SCC antigen, inhibits tumor growth with increased intratumor infiltration of natural killer cells,” *Cancer Research*, vol. 61, no. 5, pp. 1776–1780, 2001.
- [20] C. Katagiri, J. Nakanishi, K. Kadoya, and T. Hibino, “Serpin squamous cell carcinoma antigen inhibits UV-induced apoptosis via suppression of c-JUN NH2-terminal kinase,” *Journal of Cell Biology*, vol. 172, no. 7, pp. 983–990, 2006.
- [21] K. I. Hashimoto, T. Kiyoshima, K. Matsuo, S. Ozeki, and H. Sakai, “Effect of SCCA1 and SCCA2 on the suppression of TNF- $\alpha$ -induced cell death by impeding the release of mitochondrial cytochrome c in an oral squamous cell carcinoma cell line,” *Tumor Biology*, vol. 26, no. 4, pp. 165–172, 2005.
- [22] Q. Santana, V. Laura, T. Cristian et al., “SERPINB3 induces epithelial—mesenchymal transition,” *Journal of Pathology*, vol. 221, no. 3, pp. 343–356, 2010.
- [23] K. Seung-Wook, C. Kyounga, K. Chang-Hoon et al., “Proteomics-based identification of proteins secreted in apical surface fluid of squamous metaplastic human tracheobronchial epithelial cells cultured by three-dimensional organotypic air-liquid interface method,” *Cancer Research*, vol. 67, no. 14, pp. 6565–6573, 2007.
- [24] S. Tan and Z. Xiao, “Nasopharyngeal carcinoma,” *International Journal of Oncology*, vol. 34, no. 12, pp. 904–907, 2007.
- [25] K. Arai, T. Teratani, and R. Nozawa, “Immunohistochemical investigation of S100A9 expression in pulmonary adenocarcinoma: S100A9 expression is associated with tumor differentiation,” *Oncology Reports*, vol. 8, no. 3, pp. 591–596, 2001.
- [26] K. Arai, T. Yamada, and R. Nozawa, “Immunohistochemical investigation of migration inhibitory factor-related protein (MRP)-14 expression in hepatocellular carcinoma,” *Medical Oncology*, vol. 17, no. 3, pp. 183–188, 2000.
- [27] Y. Ito, K. Arai, Ryushi et al., “S100A9 expression is significantly linked to dedifferentiation of thyroid carcinoma,” *Pathology Research and Practice*, vol. 201, no. 8-9, pp. 551–556, 2005.
- [28] M. Ichikawa, R. Williams, L. Wang, T. Vogl, and G. Srikrishna, “S100A8/A9 activate key genes and pathways in colon tumor progression,” *Molecular Cancer Research*, vol. 9, no. 2, pp. 133–148, 2011.